Hindawi Publishing Corporation
Journal of Sensors
Volume 2016, Article ID 1803501, 6 pages
http://dx.doi.org/10.1155/2016/1803501

Research Article

Development of a Gastric Cancer Diagnostic Support System with a Pattern Recognition Method Using a Hyperspectral Camera

Hiroyuki Ogihara,[1] Yoshihiko Hamamoto,[1] Yusuke Fujita,[1] Atsushi Goto,[2] Jun Nishikawa,[2] and Isao Sakaida[2]

[1]*Department of Biomolecular Engineering, Yamaguchi University Graduate School of Medicine, Tokiwadai 2-16-1, Ube, Yamaguchi 755-8611, Japan*
[2]*Department of Gastroenterology and Hepatology, Yamaguchi University Graduate School of Medicine, Minami-Kogushi 1-1-1, Ube, Yamaguchi 755-8505, Japan*

Correspondence should be addressed to Yoshihiko Hamamoto; hamamoto@yamaguchi-u.ac.jp

Received 24 December 2014; Revised 3 March 2015; Accepted 16 March 2015

Academic Editor: Chao-Cheng Wu

Gastric cancer is a completely curable cancer when it can be detected at its early stage. Thus, because early detection of gastric cancer is important, cancer screening by gastroscopy is performed. Recently, the hyperspectral camera (HSC), which can observe gastric cancer at a variety of wavelengths, has received attention as a gastroscope. HSC permits the discerning of the slight color variations of gastric cancer, and we considered its applicability to a gastric cancer diagnostic support system. In this paper, after correcting reflectance to absorb the individual variations in the reflectance of the HSC, a gastric cancer diagnostic support system was designed using the corrected reflectance. In system design, the problems of selecting the optimum wavelength and optimizing the cutoff value of a classifier are solved as a pattern recognition problem by the use of training samples alone. Using the hold-out method with 104 cases of gastric cancer as samples, design and evaluation of the system were independently repeated 30 times. After analyzing the performance in 30 trials, the mean sensitivity was 72.2% and the mean specificity was 98.8%. The results showed that the proposed system was effective in supporting gastric cancer screening.

1. Introduction

Gastric cancer is a completely curable cancer when it can be detected at its early stage. Thus, because early detection of gastric cancer is important, cancer screening by gastroscopy is performed. However, about 20% of gastric cancers are reportedly missed [1], and, in addition, detection greatly depends on the physician's proficiency. Accordingly, regardless of the physician's skill, the development of diagnostic support system that provides constant diagnostic accuracy is urgently needed.

Because there is wide variability of cancer, not just in gastric cancer, even the same carcinoma can differ from person to person. Therefore, a hyperspectral camera (HSC), which can observe gastric cancer at a variety of wavelengths, has received attention [2]. The HSC has advanced the field of remote sensing. The images captured by the HSC contain 81 reflectance data values per 5 nm in the wavelength range from 400 to 800 nm for each pixel.

The HSC can discern the slight color differences of gastric cancer [3], and it is thought to be applicable to a gastric cancer diagnostic support system. However, because the color of the inner wall of the stomach varies from person to person, the individual differences in color should be absorbed to discriminate gastric cancer.

In this paper, a certain type of reflectance correction is performed to absorb the individual differences, and a system is designed using the corrected reflectance. The design of such a system involves two tasks. One is that of selecting the optimum wavelength. The HSC can observe gastric cancer

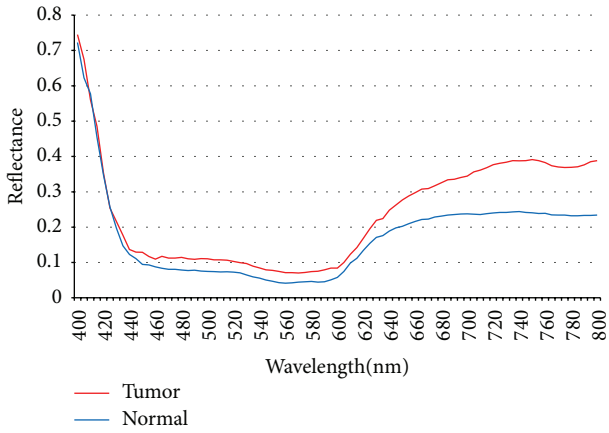

FIGURE 1: Relationship between wavelength and reflectance.

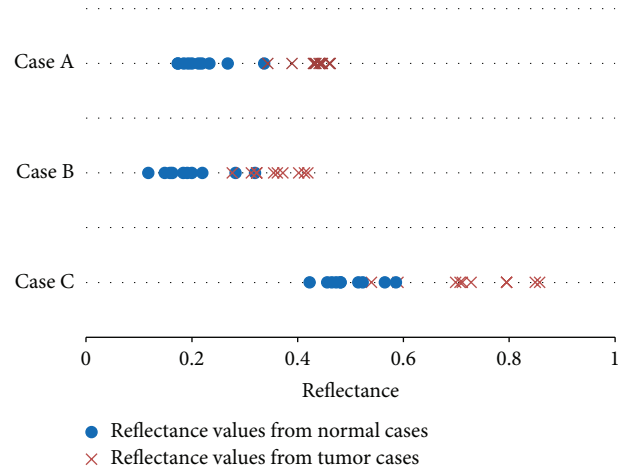

FIGURE 2: Examples of reflectance with individual differences.

with various wavelengths, but, considering cost and real-time processing, the reflectance is obtained from the optimum wavelength alone. The other task is that of determining cutoff values to distinguish gastric cancer in classifier design. These problems are solved with a pattern recognition method using training samples alone. First, with regard to the selection of the optimum wavelength, using the feature selection method in which the Mahalanobis distance [4] is defined as the criterion function, an optimum wavelength is selected from the candidate wavelengths. Next, with regard to classifier design, a minimum-distance classifier [5] is modified and used. The efficacy of the designed system is evaluated by the hold-out method [5] using test samples independent of training samples.

2. Materials and Methods

Endoscopic resections were performed in 104 cases of gastric cancer at Yamaguchi University Medical School Hospital between April 2010 and August 2012 [6], and the gastric cancers were photographed by HSC immediately after the resections. Reflectance values were measured in pairs of normal and tumor tissues in each of the 104 cases treated by endoscopic submucosal dissection. Using one of the cases as an example, Figure 1 shows the relationship between wavelength and reflectance of the normal and tumor sites, respectively. In general, the reflectance of the tumor site is larger than that of the normal site, as well as when the wavelength is greater than 650 nm, and the difference in reflectance values between the normal site and the tumor site can be clearly seen. In system design, reflectance values at 51 wavelengths between 550 nm and 800 nm were used because there is heavy overlapping between normal and tumor sites in the wavelength range from 400 to 550 nm for almost all samples. The resolution of the HSC is 480 × 640 pixels.

Because the tissue type, shape, and color of gastric tumors vary, reflectance is not always uniform even in tumor sites. Thus, 10 points were obtained from the tumor regions. The 10 points were chosen so that they were uniformly dispersed throughout the tumor as much as possible. In the same manner, 11 points obtained from the normal sites were also chosen. One of the 11 points was used for reflectance correction, and, using the remaining points, the mean of normal sites was estimated. For details of the photographs, please see [2].

2.1. Design of the Proposed System. In pattern recognition, the samples used for system design are called training samples, and those for system evaluation are called test samples. Training samples and test samples must be different [7].

Figure 2 indicates the reflectance values from normal sites with • and those from tumor sites with ×, as examples. These examples show that there are individual differences in reflectance values, in which the values sometimes indicate normal cases and other times tumor cases. These results indicate that a single cutoff value for reflectance cannot distinguish between a normal site and a tumor site. Therefore, a corrected reflectance value is used. The mean reflectance value $x^i_{(\lambda)}$ is estimated from 10 reflectance values of a normal training sample corresponding to a case i at wavelength λ. Using the mean reflectance value $x^i_{(\lambda)}$, the corrected reflectance value $X^i_{(\lambda)}$ for $x^i_{(\lambda)}$ is described as follows:

$$\begin{aligned} X^i_{(\lambda)} &= x^i_{(\lambda)} - x^i_{(\lambda)} \\ &= 0. \end{aligned} \tag{1}$$

Meanwhile, the corrected reflectance value $Y^i_{(\lambda)}$ for the mean reflectance value $y^i_{(\lambda)}$, obtained from 10 reflectance values of a tumor training sample corresponding to the case i, is described as follows:

$$Y^i_{(\lambda)} = y^i_{(\lambda)} - x^i_{(\lambda)}. \tag{2}$$

From now on, we explain the design process using the corrected reflectance values, X and Y.

First, the optimum wavelength is found. For wavelength selection, the criterion of wavelength λ is determined. The Mahalanobis distance $D_{(\lambda)}$, which represents the statistical

distance between the normal and tumor distributions, is used as the criterion:

$$D_{(\lambda)} = \frac{\left(\mu_{X(\lambda)} - \mu_{Y(\lambda)}\right)^2}{(1/2)\left(\sigma^2_{X(\lambda)} + \sigma^2_{Y(\lambda)}\right)}, \tag{3}$$

where $\mu_{X(\lambda)}$ and $\sigma^2_{X(\lambda)}$ are the respective mean and variance of the corrected reflectance value of a normal site at wavelength λ and $\mu_{Y(\lambda)}$ and $\sigma^2_{Y(\lambda)}$ are the respective mean and variance of the corrected reflectance value of a tumor site. Equation (1), $X^i_{(\lambda)} = 0$, obtained by the correction leads to

$$\begin{aligned} \mu_{X(\lambda)} &= 0, \\ \sigma^2_{X(\lambda)} &= 0. \end{aligned} \tag{4}$$

Consequently, $D_{(\lambda)}$ is as follows:

$$D_{(\lambda)} = 2\left(\frac{\mu_{Y(\lambda)}}{\sigma_{Y(\lambda)}}\right)^2. \tag{5}$$

Because there are individual differences in reflectance, using reflectance values from the normal sites in each individual, the reflectance value of the normal site is corrected by (1) and then the reflectance value of the tumor is corrected by (2). Therefore, in all of the normal training samples, the value of corrected reflectance is zero. As a pattern recognition problem, normal and tumor sites are identified as a 2-class problem. The difference in the usual 2-class problem is that the distribution of the normal class is limited to the original point by correction. For this reason, at a glance, rather than being a 2-class problem, this appears to be a 1-class problem for the tumor site.

A wavelength that maximizes the value of $D_{(\lambda)}$ is selected from 51 candidate wavelengths and is defined as the optimum wavelength $\widehat{\lambda}$. This is described as follows:

$$D_{(\widehat{\lambda})} = \max_{\lambda} D_{(\lambda)}. \tag{6}$$

Second, we explain the design process of a classifier to discriminate between pixels at the normal site and the tumor site within the images. In this paper, the minimum-distance classifier, which is the simplest classifier, is modified and used. The minimum-distance classifier assigns a pattern x to the class associated with the nearest mean value of the two classes and is described as follows:

$$\left|x - \mu_{X(\widehat{\lambda})}\right| < \left|x - \mu_{Y(\widehat{\lambda})}\right| \longrightarrow X \text{ is normal site}, \tag{7a}$$

$$\left|x - \mu_{X(\widehat{\lambda})}\right| > \left|x - \mu_{Y(\widehat{\lambda})}\right| \longrightarrow X \text{ is tumor site}. \tag{7b}$$

Here, $|a|$ is the absolute value of a. The cutoff value of this minimum-distance classifier is the midpoint, $\mu_{Y(\widehat{\lambda})}/2$, between the mean corrected reflectance value of a normal site, $\mu_{X(\widehat{\lambda})}(= 0)$, and the mean corrected reflectance value of a tumor site, $\mu_{Y(\widehat{\lambda})}$.

There is generally a trade-off relationship between sensitivity and specificity; that is, the higher the sensitivity, the lower the specificity and vice versa. Because the system is used for gastric cancer screening, a cutoff value that yields the maximum sensitivity to avoid missing cancer is expected while maintaining high specificity. A cutoff value is defined by multiplying parameters α and $\mu_{Y(\widehat{\lambda})}$, that is, $\alpha\mu_{Y(\widehat{\lambda})}$. Accordingly, optimization of a cutoff value represents optimization of parameter α. When especially $\alpha = 1/2$, this classifier becomes the minimum-distance classifier (see Figure 3).

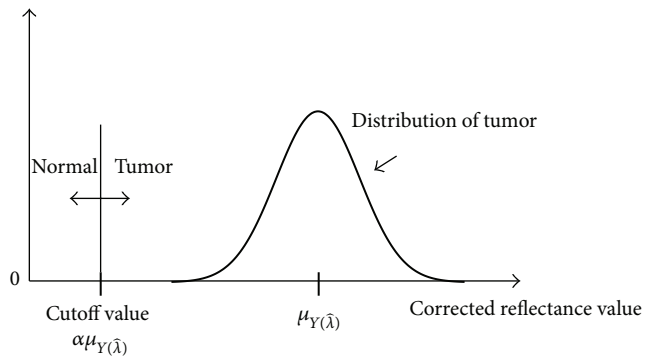

Figure 3: Modified minimum-distance classifier.

In this study, to optimize the cutoff value parameter α, we took the approach of assigning the highest value of discrimination performance to be the optimum value by actually performing discrimination. Because optimization of parameter α was performed in the classifier design stage, parameter α should be optimized using training samples alone. Thus, training samples were further divided into subtraining samples and subtest samples, and, by using subtraining samples, a classifier was designed that discriminates the subtest samples. This process was applied to each predetermined candidate value of parameter α, and, among the candidate values, a value that met the conditions of discrimination ability was selected as the optimum value $\widehat{\alpha}$. The idea of resampling the available samples as subsamples comes from the literature [8, 9]. The candidate values of parameter α were determined to be $\{1/2, 1/3, 1/4, 1/5\}$. Optimization of the parameter was conducted according to the following procedures. Procedure 5 is the condition of discrimination ability.

Procedure 1. Training samples are randomly divided into subtraining samples and subtest samples.

Procedure 2. Using subtraining samples, $\mu_{Y(\widehat{\lambda})}$ is obtained.

Procedure 3. Cutoff values are obtained using $\alpha\mu_{Y(\widehat{\lambda})}$ and $\alpha \in \{1/2, 1/3, 1/4, 1/5\}$.

Procedure 4. Using each cutoff value, subtest samples are discriminated.

Procedure 5. Regarding discrimination ability for the subtest samples, parameter α with a specificity of 99% or more and maximal sensitivity is selected as the optimum value $\widehat{\alpha}$.

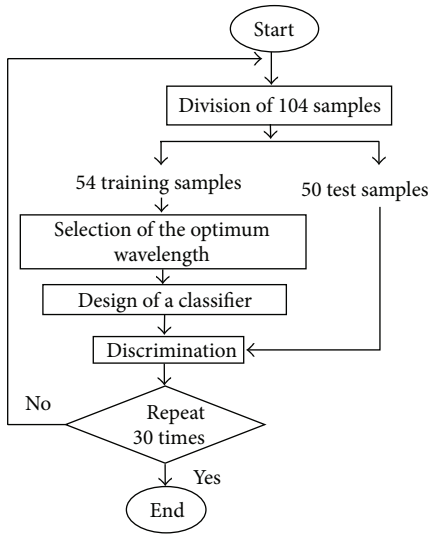

Figure 4: Flowchart of system design and assessment.

2.2. Validation of the Proposed System. The best method to evaluate the system is to assess the percentages of the sensitivity and specificity after the test samples are discriminated practically. In this paper, 104 cases were available as samples. The 104 samples were randomly divided into 54 training samples and 50 test samples, and, using the 54 training samples alone, a system was designed through which 50 test samples were discriminated. The trials described above were repeated independently 30 times, and the discrimination ability of the system was evaluated. The flowchart of the evaluation is shown in Figure 4. In addition, in parameter optimization of the cutoff values, the 54 training samples were randomly divided into 27 subtraining samples and 27 subtest samples.

In the test samples, at first, the mean value is calculated from 11 reflectance values of normal sites in the training samples, and the reflectance value that is closest to the mean value of the 11 reflectance values is selected from them as a typically normal reflectance value. The mean value of the remaining 10 reflectance values is calculated again and is defined as the mean reflectance value of normal sites. With respect to tumor sites, similar to the normal sites of the training samples, the mean value of 10 reflectance values of tumor sites is defined as the mean reflectance value of tumor sites. The corrected reflectance values of the normal and tumor sites are obtained by subtracting the typically normal reflectance values from the respective mean reflectance values.

3. Results and Discussion

Figure 5 shows the corrected reflectance values from the values in Figure 2. The reflectance values of the tumor sites are relatively larger in each case as compared with those of the normal sites. The wavelength and the value of parameter α are each acquired from 30 independent trials. With respect to the wavelength, 770 nm was chosen 11 of 30 times, and, for α, 1/4 was chosen 15 times. In this study, the most frequent wavelength was 770 nm, and 1/4 was the optimum solution. The second-rank wavelength of 675 nm was chosen 5 of 30 times, with 1/5 chosen 7 times. Also, the third-rank wavelength of 680 nm and 1/3 were chosen 3 and 4 times in 30, respectively. These are shown in Table 1.

Figure 5: Examples of corrected reflectance values for training samples.

Table 1: $\widehat{\lambda}$ and $\widehat{\alpha}$ values with the highest frequencies of selection.

	First rank	Second rank	Third rank
Optimum wavelength $\widehat{\lambda}$	770 nm	675 nm	680 nm
Optimum parameter $\widehat{\alpha}$	1/4	1/5	1/3

Table 2: Discrimination ability of the system using 770 nm and 1/4 for test samples.

Rate of discrimination (%)	Sensitivity (%)	Specificity (%)	Youden index
85.5	72.2	98.8	0.710
[84.6, 86.4]	[70.5, 73.9]	[98.4, 99.2]	[0.692, 0.728]

The numbers in the upper row indicate the mean values, and the numbers in the lower row indicate the 95% confidence interval.

The results of the discrimination with the use of 770 nm and 1/4 are shown in Table 2. Within the 30 discrimination trials, the mean sensitivity and specificity were 72.2% and 98.8%, respectively. Also, the Youden index [10], which is defined as sensitivity + specificity − 1, is shown for reference. High specificity is needed for gastric cancer screening, and sensitivity must also be high so that no cancer is missed. Although a sensitivity of 72.2% seems to be low, the discrimination in this study is conducted for each pixel, and, thus, despite the low sensitivity of each discrimination, pixels that are discerned as cancer congregate to form one region within the image, leading to avoidance of missing cancer by the physician.

The point of this study can be found in the correction of individual differences of reflectance. Therefore, to clarify the effects of this correction, we conducted an experiment

Table 3: Discrimination ability with and without correction.

	Optimum wavelength	Optimum parameter	Rate of discrimination (%)	Sensitivity (%)	Specificity (%)	Youden index
With correction	770 nm	1/4	85.5	72.2	98.8	0.710
Without correction	780 nm	1/5	67.0	73.8	60.2	0.340

Table 4: Effect of an increase in the number of features.

Wavelength	Optimum parameter	Rate of discrimination (%)	Sensitivity (%)	Specificity (%)	Youden index
770 nm	1/4	85.5	72.2	98.8	0.710
770 nm, 675 nm	1/4	86.4	74.9	97.9	0.729

comparing techniques that perform correction with techniques that do not perform correction. In both techniques, feature selection was performed using the Mahalanobis distance, and the modified minimum-distance classifier was used. As shown in Table 3, when comparing with and without correction, discrimination ability was improved with correction, and, accordingly, the validity of the correction was revealed.

We used only one wavelength for discrimination in our original study. Therefore, we conducted an experiment to determine whether discrimination performance could be improved by increasing the number of wavelengths. Specifically, the discrimination experiment was conducted on two-dimensional feature space by combining the optimum wavelength of 770 nm and the second-rank wavelength of 675 nm. The results are shown in Table 4. Even when the number of features was increased, the discrimination performance remained virtually unchanged. By using the value of the Youden index, hypothesis tests were conducted of the differences in average value with respect to the performance of 770 nm independently and the combined performance of 770 nm and 675 nm, and there was no significant difference in the results of either test ($P = 0.13$).

Real-time processing was required in this study. Not only does increasing the number of features lengthen the processing time, but also the hardware scale increases. Since no clear improvement in discrimination performance is obtained by increasing the number of features, by emphasizing the real-time processing, we have adopted a one-dimensional system by using one wavelength. For practical use, there may be a problem with the photographic speed of the HSC, which photographs at many wavelengths. However, since the system uses a single optimum wavelength, the photographic speed of the HSC does not matter, and thus real-time processing is achievable.

Finally, when this system is applied in practical use, correction will be a problem. Correction requires normal samples, but such samples are not actually available. Therefore, in this paper, we hypothesize that when the camera photographs the inside of the stomach, almost all of the pixels within the image will be normal pixels. If the image contains many pixels of cancer, a doctor can easily detect cancer without the support of the system. In general, this hypothesis is considered to be formed for the images used for gastric cancer screening. If this hypothesis is satisfied, one pixel is randomly selected within the images and can be used as a normal pixel for correction.

This research depends on the data that is acquired. This means that the individual wavelength and cutoff value should be optimized depending on the hyperspectral camera that is used. Therefore, the values of 770 nm and 1/4 might not be valid when another hyperspectral camera is used. However, as revealed in this study, to resolve the problem of individual differences in patients, the value of this study is in establishing an approach whereby real-time processing is possible.

4. Conclusion

In this paper, we developed a diagnostic support system for gastric cancer that could discern between a pixel of a normal site and a pixel of a tumor site for each pixel in the images of 104 gastric cancer cases photographed by a HSC. Based on the results of 30 independent trials with the optimal wavelength 770 nm and cutoff value of 1/4, it was shown that this system is effective in screening for gastric cancer, achieving an average sensitivity of 72.2% and average specificity of 98.8%.

From the standpoint of this study, whether a lesion is gastric cancer is ultimately determined by the physician, and the system supports the physician to avoid missing gastric cancer. For this purpose, the system can discriminate on a pixel-by-pixel basis and support a physician's interpretation with a color display of the regions consisting of pixels discriminated as a tumor in the images.

The data used here are from images of tissues photographed by the HSC immediately after gastric cancer resection. In the future, we aim to use the system in the clinical setting, and we are planning to perform experiments using images photographed from within the stomach.

Conflict of Interests

The authors declare that there is no conflict of interests regarding the publication of this paper.

References

[1] K. Aida, H. Yoshikawa, C. Mochizuki et al., "Clinicopathological features of gastric cancer detected by endoscopy as part

of annual health checkup," *Journal of Gastroenterology and Hepatology*, vol. 23, no. 4, pp. 632–637, 2008.

[2] S. Kiyotoki, J. Nishikawa, T. Okamoto et al., "New method for detection of gastric cancer by hyperspectral imaging: a pilot study," *Journal of Biomedical Optics*, vol. 18, no. 2, Article ID 026010, 2013.

[3] S. Satori, Y. Aoyanagi, U. Hara, R. Mitsuhashi, and Y. Takeuchi, "Hyperspectral sensor HSC3000 for nano-satellite TAIKI," in *2nd Multispectral, Hyperspectral, and Ultraspectral Remote Sensing Technology, Techniques, and Applications*, vol. 7149 of *Proceedings of SPIE*, p. 71490M, Noumea, New Caledonia, November 2008.

[4] R. O. Duda, P. E. Hart, and D. G. Stork, *Pattern Classification*, John Wiley & Sons, 2nd edition, 2001.

[5] K. Fukunaga, *Introduction to statistical pattern recognition*, Computer Science and Scientific Computing, Academic Press, Boston, Mass, USA, 2nd edition, 1990.

[6] A. Goto, J. Nishikawa, S. Kiyotoki et al., "Use of hyperspectral imaging technology to develop a diagnostic support system for gastric cancer," *Journal of Biomedical Optics*, vol. 20, no. 1, Article ID 016017, 2015.

[7] S. J. Raudys and A. K. Jain, "Small sample size effects in statistical pattern recognition: Recommendations for practitioners," *IEEE Transactions on Pattern Analysis and Machine Intelligence*, vol. 13, no. 3, pp. 252–264, 1991.

[8] B. Efron and R. J. Tibshirani, *An Introduction to the Bootstrap*, Chapman & Hall, 1993.

[9] Y. Hamamoto, S. Uchimura, and S. Tomita, "A bootstrap technique for nearest neighbor classifier design," *IEEE Transactions on Pattern Analysis and Machine Intelligence*, vol. 19, no. 1, pp. 73–79, 1997.

[10] W. J. Youden, "Index for rating diagnostic tests," *Cancer*, vol. 3, no. 1, pp. 32–35, 1950.